LIMNOLOGY and OCEANOGRAPHY

ASLO

Limnol. Oceanogr. 9999, 2024, 1–13

doi: 10.1002/lno.12667

Causal feedback loops modify lake chlorophyll *a*–nutrient relationships over two decades of nutrient reductions and climate warming

Hui Fu,[1*] Korhan Özkan,[2] Liselotte Sander Johansson,[3] Martin Søndergaard,[3,4] Torben Linding Lauridsen,[3,4] Guixiang Yuan,[1*] Erik Jeppesen[2,3,4,5]

[1]Department of Ecology, College of Environment & Ecology, Hunan Provincial Key Laboratory of Rural Ecosystem Health in Dongting Lake Area, Hunan Agricultural University, Changsha, China
[2]Institute of Marine Sciences, Middle East Technical University, Erdemli-Mersin, Turkey
[3]Department of Ecoscience and Water Technology Centre/WATEC, Aarhus University, Aarhus, Denmark
[4]Sino-Danish Centre for Education and Research (SDC), University of Chinese Academy of Sciences, Beijing, China
[5]Limnology Laboratory, Department of Biological Sciences and Centre for Ecosystem Research and Implementation, Middle East Technical University, Ankara, Turkey

Abstract

Understanding how the causal feedback between phytoplankton and environmental drivers controlling the chlorophyll *a* (Chl *a*, as a proxy of phytoplankton biomass)–nutrient relationships are modulated under different ecosystem conditions is a major challenge in aquatic ecology. Using an empirical dynamic model (convergent cross mapping) on a 20-yr dataset on 20 Danish lakes, we quantified hypothesized causal feedback networks for each lake and related them to lake system properties (e.g., mean water depth, nutrient concentrations and extent of reduction, climate warming) vs. the Chl *a*–nutrient relationship (estimated from generalized least square models). The results showed prevalent causal feedback across the studied lakes, which demonstrated clear patterns for the tested ecosystem variations. Weaker causal feedbacks were found in deeper lakes and lakes with larger warming trends, while stronger causal feedbacks appeared in lakes experiencing greater reductions of TP (total phosphorus) and TN (total nitrogen). Moreover, these causal feedbacks showed a strong and positive coupled pattern. Most of the causal feedbacks worked as enhancement loops, which promote the sensitivity of phytoplankton to TP, not least in shallow lakes with a high TP reduction, and as regulatory loops, which force a shift in the Chl *a*–TN relationship from a more negative slope in lakes experiencing a high nutrient reduction and weak warming to a positive slope in lakes with low nutrient reduction and stronger warming. Our findings suggest a mechanistic explanation of how internal feedbacks regulate the Chl *a*–nutrient relationships across a broad gradient of nutrient reductions, climate warming, and lake morphologies.

The mechanisms driving chlorophyll *a* (Chl *a*) (used as a proxy of phytoplankton biomass)–nutrient relationships are fundamental for freshwater ecosystem function and, therefore, important to elucidate for lake managers (Smith and Schindler 2009). Based on Liebig's law, numerous empirical and experimental studies have found that phosphorus (P) and nitrogen (N) are the primary factors limiting phytoplankton growth and thus Chl *a* concentrations in lakes (McCauley et al. 1989; Prairie et al. 1989; Phillips et al. 2008; Filstrup et al. 2014; Quinlan et al. 2021). Therefore, a reduction of the loading of either P or both N and P has been recommended to mitigate eutrophication worldwide (Paerl and Otten 2013*b*; Paerl et al. 2016; Schindler et al. 2016). However, the Chl *a*–nutrient relationship is highly context-dependent (e.g., lake type, trophic status etc.) and comes with great uncertainty (Canfield et al. 2019; Olson and Jones 2022; Zhao et al. 2023).

The Chl *a*–TP relationship follows a log-linear pattern at intermediate P concentrations and displays a sigmoid pattern at larger P gradients (Quinlan et al. 2021), while wedge-shaped scatter diagrams widely suggest a high degree of Chl *a* variability between lakes at a given nutrient level (Cade and Noon 2003; Canfield et al. 2019). This variability may, in part be caused by a variety of ecosystem differences in lake morphology, chemistry, and climate at local regional and global scales (Quinlan et al. 2021; Wu et al. 2022; Zou et al. 2022; Zhao et al. 2023). At the local scale, deeper and stratified lakes

*Correspondence: fuhui@hunau.edu.cn and yuangx987@hunau.edu.cn

Additional Supporting Information may be found in the online version of this article.

Author Contribution Statement: HF and GY conceived and designed the research. LS, MS, TL, and EJ collected the data. KÖ and HF performed the data curation. HF analyzed the data. HF, GY, and EJ wrote and edited the manuscript and others made the revisions.

exhibit low Chl *a* per unit of nutrients and lakes with high transparency generally have low Chl *a* concentrations at a given nutrient level, while shallow lakes with low and moderate alkalinity have the highest Chl *a* levels (Phillips et al. 2008; Zhao et al. 2023). High salinity and acidic water limit P bioavailability, leading to lower Chl *a* per unit of nutrients (Prepas and Trew 1983). Phytoplankton is more sensitive to TN at high TP levels (Zhao et al. 2023). Large zooplankton (e.g., *Daphnia*) may weaken the Chl *a*–TP relationship through grazer control of phytoplankton biomass (Jeppesen et al. 2005*a*, 2011; Wu et al. 2022). At the regional scale, the rate at which Chl *a* increases with nutrients is strongly related to watershed-specific characteristics, the Chl *a*–TP relationship being higher in regions with less wetland cover and richer pasture fields (Filstrup et al. 2014). Filstrup et al. (2014) further found a weaker relationship at the annual temperature extremes ($< -5°C$ and $> 25°C$) and dominance of lake- and watershed-specific characteristics within the moderate temperature range, and according to Zou et al. (2022) the sensitivity of Chl *a* to nutrients is strongly influenced by changes in temperature, water level, wind speed, the N : P mass ratio and grazing pressure. Furthermore, the regional meteorology might be causally linked with the global climate oscillation (e.g., El Niño, the Southern Oscillation, North Atlantic Oscillation) and thus potentially show teleconnections with local biotic (e.g., phytoplankton and zooplankton) and abiotic (e.g., temperature, stratification onset) environments in both subtropical and temperate lakes (Arhonditsis et al. 2004; Winder and Schindler 2004*a*; Blenckner et al. 2007; Xiao et al. 2019; Fu et al. 2022). However, the intrinsic mechanisms responsible for the observed patterns have yet to be fully elucidated.

Phytoplankton not only responds to varying nutrient levels, but it also has feedback to the nutrient cycling (Paerl and Otten 2013*a*; Cottingham et al. 2015). Thus, phytoplankton alters the abundance of dissolved nutrients by direct uptake and then returns inorganic nutrients to the water after death (Carpenter et al. 1992). In addition, phytoplankton may indirectly affect the nutrient dynamics through alterations in the local environment (Gao et al. 2014; Cottingham et al. 2015). For instance, phytoplankton blooms increase pH and organic matter concentrations, increase oxygen depletion in the bottom water and reduce water transparency (i.e., Secchi depth, SD), stimulate P release from the sediment and N loss by denitrification, all of which increase the rate and magnitude of the internal nutrient recycling (Cottingham et al. 2015; Huisman et al. 2018; Fu et al. 2024). Such phytoplankton-dominant feedbacks could form enhancement loops where a minor increase in nutrient levels leverages extensive phytoplankton proliferation (Scheffer et al. 1993; Fu et al. 2024), leading to enhanced sensitivity of phytoplankton to nutrients. Accordingly, recent studies have demonstrated that climate warming, especially during winter, and atmosphere stilling increase phytoplankton sensitivity to nutrients and thus exacerbate eutrophication by strengthening the self-amplifying feedback loops (Yan et al. 2017; Deng et al. 2018; Qin et al. 2019; Meerhoff et al. 2022; Fu et al. 2024). However, these feedback loops might differ greatly depending on lake morphology, nutrient input, and macrophyte cover (Yuan and Jones 2020; Meerhoff et al. 2022). Therefore, the feedback loops involving phytoplankton and nutrients, as well as their drivers might play an important mechanistic role in modifying Chl *a*–nutrient relationships in diverse habitats.

Feedback loops have been suggested to be important internal forces in maintaining ecological stability in ecosystems (Scheffer et al. 1993), which could be identified as both unidirectional (triple feedbacks: $A \rightarrow B \rightarrow C \rightarrow A$) or bidirectional pairwise feedbacks: ($A \leftrightarrow B$) causality that forms a closed cycle. The strength of the feedback loops is spatially and temporally variable and thus frequently difficult to quantify with traditional linear statistics (e.g., correlation, regression, structural equation model), especially in a dynamic ecosystem (Chang et al. 2022; Fu et al. 2024). Convergent cross mapping (CCM) is an empirical dynamic model that can help to detect distinct causal interaction structures (unidirectional or bidirectional causality) from spurious correlations in time series (e.g., population and environment timeseries in ecology research) in dynamic systems (Sugihara et al. 2012).

Here, based on a 20-yr dataset from 20 Danish lakes, we used CCM (Sugihara et al. 2012) to construct causal feedback networks for each of our study lakes in order to assess how causal feedback altered Chl *a*–nutrient relationships during a period in which the lakes faced both re-oligotrophication and climate warming. We evaluated the strength of the causal feedback between phytoplankton and the tested drivers (e.g., local nutrients, regional meteorology, and global climate oscillation) and related them to lake system properties (e.g., water depth, long-term trends in temperature and nutrients) and the Chl *a*–nutrient relationship (estimated from generalized least square models). We addressed the following questions: (1) How do phytoplankton interact with the drivers and what is the magnitude of the phytoplankton feedback to these drivers? Are these causal feedbacks common in the studied lake ecosystems? (2) How do causal feedbacks vary in strength across lake ecosystems? Especially when these lakes have undergone distinct magnitudes of changes in nutrients and climate warming. (3) How do causal feedbacks govern the Chl *a*–nutrient relationship? Among these causal feedbacks, specifically, which ones are characterized by enhancement loops that boost phytoplankton responses to nutrients and which ones are regulatory loops that reduce phytoplankton responses to nutrients.

Materials and methods

Data collection

We used a long-term (1989–2008) monitoring dataset on 20 lakes included in the Danish National Monitoring Programme on the Aquatic Environment, NOVANA (Supporting

Information Fig. S1). The average sampling interval of the lakes was 14 d from May to October and 30 d in the other months. Details on measurements of abiotic variables, phytoplankton and zooplankton sampling, identification, and data curation can be found in Özkan et al. (2014) and Fu et al. (2020). To construct the hypothesized feedback networks for each lake (Supporting Information Fig. S1), we used local variables, including Chl *a*, nitrate (NO_3), orthophosphate (PO_4), ammonium (NH_4), Secchi depth (SD), pH and zooplankton biomass (zbiomass), and regional variables, encompassing precipitation (Precip), wind speed (WindSpeed), air temperature (AirTemp) and solar irradiance (Light). We also included global climatic oscillations such as the El Niño, the Southern Oscillation (ENSO), the Pacific Decadal Oscillation (PDO), North Atlantic Oscillation (NAO), and the Atlantic Multidecadal Oscillation (AMO). Total phosphorus (TP) and total nitrogen (TN) were used to assess the phytoplankton response to nutrients (log-linear Chl *a*–nutrient relationships). All the tested variables were monthly averaged ($n = 240$). For each time series (variables) in each lake, we used the residuals from a linear regression against time to eliminate temporal linear trends and ensure stationarity. Furthermore, the time series were de-seasonalised by scaling them against the mean and standard deviation of values occurring in the same month across the studied periods (Fu et al. 2024).

Data analysis

At the individual lake scale (*Question 1*), we first evaluated whether there were significant causal feedbacks between Chl *a* and tested variables (i.e., local, regional, and global) according to an empirical dynamic causality analysis—convergent cross mapping (CCM) (Takens 1981; Sugihara et al. 2012). We then quantified the strength of causal feedback as the geometric mean (i.e., Neutel's loop weight) of SLS for all linkages (*Question 1*) (Chang et al. 2022). Using a generalized least squares model (GLS) with temporal autoregressive error structures (*corArma* function), we estimated Chl *a*–nutrient (TP and TN) relationships separately for each lake. Therefore, we yield one value for the strength of each casual feedback and for the slope of the Chl *a*–nutrient relationship, respectively, for each lake.

Across the lakes, the strength of the two distinct causal feedbacks that are calculated from CCM for each lake was compared through permutation analysis, and the coupling between them, as well as between each causal feedback and the lake-level property, was identified with Spearman correlation analysis (*Question 2*). To assess how these causal feedbacks control the Chl *a*–nutrient relationships (*Question 3*), we first tested if there was a significant correlation between them using Spearman correlation analysis and then quantified the relative importance of the remaining significant determinants using Random Forest (RF) analysis. Then, we modeled the multiple relationships between lake-level properties, the strength of causal feedbacks, and the Chl *a*–nutrient relationships using generalized multilevel path models (GMPMs; *Question 3*) (Shipley 2009).

Convergent cross mapping (CCM)

The CCM approach is based on Takens' theorem for dynamical systems, which states that the historical information of causal variable (Y) is encoded in the time series of the effector variable (X) if X and Y are part of the same dynamical system (Takens 1981). That is, the reconstructed state spaces of X and Y topologically represent the same attractor (with a one-to-one mapping between the reconstructed attractors of X and Y). For this point, CCM could quantify the information transfer from X to Y by reconstructing their nonparametric state space when a causal association exists between the two variables, and the causal direction depends on the direction of the information flow (Sugihara et al. 2012). The strength of causal feedback between pairs of time series was defined as the correlation coefficient ρ (hereafter called "cross-map skill") between estimated states of Y from states of X and actual observations of Y (Sugihara et al. 2012). Therefore, CCM has been suggested to have a great ability to detect the mirage correlations (i.e., the sign and magnitude of the correlation vary with time) between two variables in complex nonlinear dynamic systems (Sugihara et al. 2012). Details about CCM analysis and procedures for significance testing causal links are described in Supporting Information Methods. For the distinct paths mapped in Supporting Information Fig. S1, the significant path ($A \rightarrow B$) revealed by CCM was considered as causal linkages, the significant bidirectional path ($A \rightarrow B$ and $B \rightarrow A$) as causal pairwise feedback loop, the significant directed cyclic loop ($A \rightarrow B \rightarrow C \rightarrow A$: $A \rightarrow B$, $B \rightarrow C$, $C \rightarrow A$) as causal triple feedback loop, and the significant unidirectional loop with two paths ($A \rightarrow B \rightarrow C$: $A \rightarrow B$, $B \rightarrow C$) as a causal pathway. The paths work as enhancement (or self-reinforced, self-amplified) loops if they increase the Chl *a*–nutrient relationship (promote the response of phytoplankton to nutrients) and as regulatory loops if they decrease the Chl *a*–nutrient relationship.

Strength of causal feedback loops at individual lake scale

The strength of causal feedback was firstly determined as a cross-mapping skill at maximal library size ($\rho(L_{max})$). Notably, the $\rho(L_{max})$ for each causal feedback was standardized by dividing linkage strength (SLS) by the maximum $\rho(L_{max})$ within each lake, which was used to exclude systematic noise in cross-mapping skill (ρ) among lakes (Chang et al. 2022). The SLS ranged from 0 to 1, and a larger value indicated a stronger causal effect. For each lake, the hypothesized causal feedback networks were mapped (Supporting Information Fig. S1), and then the $\rho(L_{max})$ was standardized separately for each lake (Fu et al. 2024).

The strength of the causal feedback was quantified separately for pairwise and triple ones. For each hypothesized causal feedback, we calculated the geometric mean (i.e., Neutel's loop

weight) of SLS for all linkages (Chang et al. 2022). For example, the loop weight for pairwise feedback ($A \leftrightarrow B$) is determined as the geometric mean of the SLS in both directions (i.e., $A \rightarrow B$ and $B \rightarrow A$), while triple feedback is determined as the geometric mean of the SLS in a directed cyclic loop with all three paths (i.e., type I: $A \rightarrow B \rightarrow C \rightarrow A$; type II: $A \rightarrow C \rightarrow B \rightarrow A$) (Fu et al. 2024). Likewise, the geometric mean of the SLS for all causal feedbacks in the pathway (i.e., $A \rightarrow B \rightarrow C$) was calculated as the causal effects of global climate oscillation on the components of the local feedback loops through meteorological variables (Fu et al. 2024). To assess the uncertainty associated with our estimations of loop weight, we generated 500 random samples by resampling the embedded data points with replacement and then determined their standard errors from the reconstructed sampling distributions (Chang et al. 2022).

Chl *a*–nutrient relationships at individual lake scale

To assess the Chl *a*–nutrient (TP and TN) relationship separately for each lake, we used a generalized least squares model (GLS) with temporal autoregressive error structures (i.e., *corArma* function). The GLS slope is as proxy for the Chl *a*–nutrient (TP, TN) relationship in the subsequent analysis.

Relating the causal feedback loops and Chl *a*–nutrient relationships across lakes

We used four lake-level properties characterizing physical environments (mean water depth), re-oligotrophication (TP_tau and TN_tau), and climate warming (AT_tau), where "tau" indicates the coefficients estimated from Kendall's τ test over time for each variable during the 20 yr of monitoring.

We conducted a permutation test with a sample size of 9999 to compare the strength (SLS) of the two significant and distinct causal feedbacks (e.g., $PO_4 \rightarrow$ Chl *a* vs. $NO_3 \rightarrow$ Chl *a*) or feedback loops (e.g., pairwise: $NH_4 \leftrightarrow$Chl *a* vs. $PO_4 \leftrightarrow$Chl *a*, triple: $NH_4 \rightarrow$ Chl *a* $\rightarrow$ pH $\rightarrow NH_4$ vs. $PO_4 \rightarrow$ Chl *a* $\rightarrow$ pH $\rightarrow PO_4$), which were permutated randomly across 20 lakes ($N = 20$). Moreover, Spearman correlation analyses were employed to examine the relationships between the strength of distinct causal feedbacks (e.g., linkages, pairwise, triangle, pathway), respectively. In addition, we assessed the Spearman correlation between the strength of causal feedback and the four lake-level systematic properties: mean water depth, TP_tau, TN_tau, and AT_tau.

Random Forest regression in combination with Spearman correlation was applied to assess the importance of the identified causal feedback in influencing the Chl *a*–nutrient relationship. Random Forest regression, incorporating a bootstrapping classification tree (Breiman 2001), not only addresses overfitting but also effectively manages spatial autocorrelation among samples (Breiman 2001). For each Chl *a*–TP and Chl *a*–TN relationship, we initially identified their significant determinants through Spearman correlation. Specifically, $NH_4 \leftrightarrow$ Chl *a*, zbiomass $\leftrightarrow$ Chl *a*, $NH_4 \rightarrow$ Chl *a* $\rightarrow$ pH $\rightarrow NH_4$, $NH_4 \rightarrow$ Chl *a* $\rightarrow$ SD $\rightarrow NH_4$, and $NH_4 \rightarrow$ Chl *a* $\rightarrow$ zbiomass $\rightarrow NH_4$ were retained for Chl *a*–TP, while pH $\leftrightarrow$ Chl *a*, $NO_3 \leftrightarrow$ Chl *a*, $NO_3 \rightarrow$ pH $\rightarrow$ Chl *a* $\rightarrow NO_3$, Chl *a* $\rightarrow NO_3$, $NO_3 \rightarrow$ Chl *a* $\rightarrow$ zbiomass $\rightarrow NO_3$, and ENSO $\rightarrow$ AirTemp $\rightarrow$ Chl *a* were retained for Chl *a*–TN. These determinants were then included in the Random Forest regression model as potential predictors, randomly resampled to create 500 unpruned decision trees. The relative importance of each variable was quantified by the percentage increase in mean standard error (MSE) for the Random Forest regression model predictions. To gauge uncertainty of Random Forest regression, we calculated a prediction uncertainty metric (e.g., conditional mean squared biases) based on a novel estimator of the conditional prediction error distribution function (Lu and Hardin 2021).

We applied generalized multilevel path models (GMPMs) to specify how the strength of the causal feedbacks modified the Chl *a*–nutrient relationship with systematic differences in lake morphology, the magnitude of re-oligotrophication and climate warming (Shipley 2009). The generalized multilevel path models were fitted separately for Chl *a*–TP and Chl *a*–TN. The generalized multilevel path models are the most proper method when dealing with ecological monitoring data that are characterized by non-normal distribution and temporal and spatial dependence (Shipley 2009). Our generalized multilevel path models included three sets of hypothesized paths: (1) lake systematic properties influencing the strength of the causal feedbacks; (2) lake systematic properties influencing the Chl *a*–nutrient relationship; (3) how the causal feedbacks govern the Chl *a*–nutrient relationship. In addition, we included correlations between the different causal feedbacks because their directions were not hypothesized. For each component model of generalized multilevel path models, we applied linear models to fit the predictors. We tested if there was collinearity in the explanatory variables for each path model by estimating variance inflation factors (O'brien 2007), and all variables had variance inflation factors < 7. We examined the goodness of fit using Shipley's test of directional separation (Shipley 2009) and the significance using Fisher's *C* test for each path model (Shipley 2013), and the best model was selected using the AICc procedure (Shipley 2013). We used standardized path coefficients to present the path effects of the predictors (Grace and Bollen 2005).

All statistical analyses were conducted using R version 4.12 software (R Core Team 2013). Cross-correlation mapping (CCM) was executed with the "*rEDM*" package (https://github.com/SugiharaLab/rEDM) in R (v-0.7.5) (Ye et al. 2016). Concise animations illustrating the fundamental concepts of CCM can be found at tinyurl.com/EDM-intro, while comprehensive guidelines for performing EDM analyses are available at https://deepeco.ucsd.edu/resources/#pagecontent. Kendall's τ test was implemented using the *mann-kendall* function within the "*kendall*" package. Random Forest models were run using the "*randomForest*," "*rfPermute*," "*A3*" package, generalized multilevel path models were conducted employing the

"*piecewiseSEM*" package (Lefcheck 2016), and visual representations were generated with the "*ggplot2*" package.

Results

The 20 lakes studied varied greatly in morphology (mean and maximum water depth) and nutrient conditions (TP and TN), and most lakes experienced remarkable reductions in TP and TN and a rise in air temperature during the study period despite their distinct magnitudes of temporal trends (Supporting Information Table S1).

Based on CCM analysis (Supporting Information Table S2), we found significant causal effects of the local and regional drivers on Chl *a* for most lakes as well as significant causal feedbacks of Chl *a* to the local environments. The permutation test showed that Chl *a* was most responsive to Secchi depth, followed by pH and NO_3 (Fig. 1a, all $p < 0.001$), and the averaged strengths for the causal effects of PO_4, NH_4, and zbiomass were comparable (Fig. 1a, $p > 0.05$). Similar patterns were observed for the opposite directions (Fig. 1b, i.e., Chl $a \rightarrow$ environments) as well as for the pairwise feedback between Chl *a* and the local drivers (Fig. 1c).

The causal effects of regional drivers on Chl *a* (e.g., AirTemp, Precip, WindSpeed) were notably inferior to those exhibited by local drivers (Fig. 1d, all $p < 0.01$), except for light (comparable to PO_4). Notably, we also found non-negligible causal effects from global climate oscillation to Chl *a* via the regional drivers, though their strengths were generally low (SLS < 0.4). The physicochemical and nutrient-associated triple feedback loops were much stronger than the zooplankton-associated ones (Fig. 1e,f, all $p < 0.05$).

The strength of causal feedback varied significantly with water depth, TP_tau, TN_tau, and AT_tau (Table 1). Among the tested causal feedbacks, 13 (including 2 marginally) causal feedbacks decreased significantly in the loop weight toward deep lakes, 14 (6 marginally), and 6 (4 marginally) causal feedbacks increased significantly in the loop weight in lakes undergoing large reductions of TP and TN, respectively, and 17 (6 marginally) causal feedbacks decreased significantly in the loop weight in lakes experiencing strong increases in air temperature (Table 1). Remarkably, the Spearman correlation analysis demonstrated a strong and positive coupled pattern between 82% causal linkages (Supporting Information Fig. S2A), 89% pairwise (Supporting Information Fig. S2B), and 94% triangle (Supporting Information Fig. S2C) feedbacks and 85% causal pathways (Supporting Information Fig. S2D).

Using the GLS model, we observed that 17 and 15 lakes, respectively, had significant log-linear Chl *a*–TP and Chl *a*–TN relationships (Table 2). The GLS slope of Chl *a*–TP was mostly positive (0.01–1.03), except for Lake SOHOLM SO (−0.44), and that of Chl *a*–TN ranged from −1.03 to 1.48. The Random Forest regression models revealed that the feedbacks between Chl *a* and NH_4, zbiomass were generally important for prompting the GLS slope of Chl *a*–TP (Fig. 2a), while pH, NO_3- and temperature-associated feedbacks were highly important in decreasing the GLS slope of Chl *a*–TN (Fig. 2b). The prediction error was low for Chl *a*–TP (conditional mean squared biases = −0.046) and Chl *a*–TN (conditional mean squared biases = −0.088).

According to the AICc model selection procedure, the final GMPMs explained 90% of the variation of the Chl *a*–TP slope (Fig. 3a; $\chi^2 = 9.35$, df = 16, $p = 0.90$, AICc = −197.83) and 62% of the variation of the Chl *a*–TN slope (Fig. 3b; $\chi^2 = 14.94$, $df = 20$, $p = 0.78$, AICc = −329.96). The three retained causal feedbacks ($NH_4 \leftrightarrow$ Chl *a*, $NH_4 \rightarrow$ Chl $a \rightarrow$ pH $\rightarrow NH_4$, Chl $a \rightarrow$ zbiomass) increased the Chl *a*–TP slope (Figs. 3a, 4). The mean water depth of lakes decreased the Chl *a*–TP slope either directly or indirectly through changes in the strengths of the causal feedback. Climate warming trends (more positive AT_tau) decreased the Chl *a*–TP slope indirectly through changes in the strength of $NH_4 \rightarrow$ Chl $a \rightarrow$ pH $\rightarrow NH_4$, while TP reduction trends (more negative TP_tau) increased the Chl *a*–TP slope indirectly through changes in the strength of $NH_4 \rightarrow$ Chl $a \rightarrow$ pH $\rightarrow NH_4$ and $NH_4 \leftrightarrow$ Chl *a*.

The bidirectional feedback between $PO_4 \leftrightarrow$ Chl *a* increased, and $NO_3 \leftrightarrow$ Chl *a* and pH $\leftrightarrow$ Chl *a* decreased the Chl *a*–TN slope (Figs. 3b, 5). TN reduction trends (more negative TN_tau) directly enhanced the Chl *a*–TN slope, while TP reduction trends (more negative TP_tau) indirectly promoted it through changes in the strength of $PO_4 \leftrightarrow$ Chl *a* and pH $\leftrightarrow$ Chl *a*. Climate warming trends (more positive AT_tau) indirectly decreased the Chl *a*–TN slope via changes in the strength of $PO_4 \leftrightarrow$ Chl *a* and $NO_3 \leftrightarrow$ Chl *a*.

Discussion

The key variables describing ecosystem dynamics are highly interdependent and extensively interactive, and they often interact in a nonlinear state-dependent way to form dynamic interactions. Using a two-decade dataset on 20 Danish lakes, we applied empirical dynamic modeling (e.g., CCM) to reconstruct and quantify the causal feedback loops between Chl *a* and the tested drivers for each lake. Predominantly bidirectional causal linkages were identified, supporting the hypothesis that causal feedbacks occur commonly in the studied lake ecosystems. Our results highlighted that the tested causal feedback played an important role in modifying the Chl *a*–nutrient relationships in response to distinct system properties.

The common bidirectional causal feedback between phytoplankton and local drivers was significant (Supporting Information Tables S2–S4) across the 20 Danish lakes covering a broad range of nutrients and morphology (Supporting Information Table S1). This provides evidence that phytoplankton can be controlled not only by a variety of local and regional drivers, but that it may also have important feedback on the physicochemical environment, nutrient recycling, and zooplankton, forming prevalent pairwise or

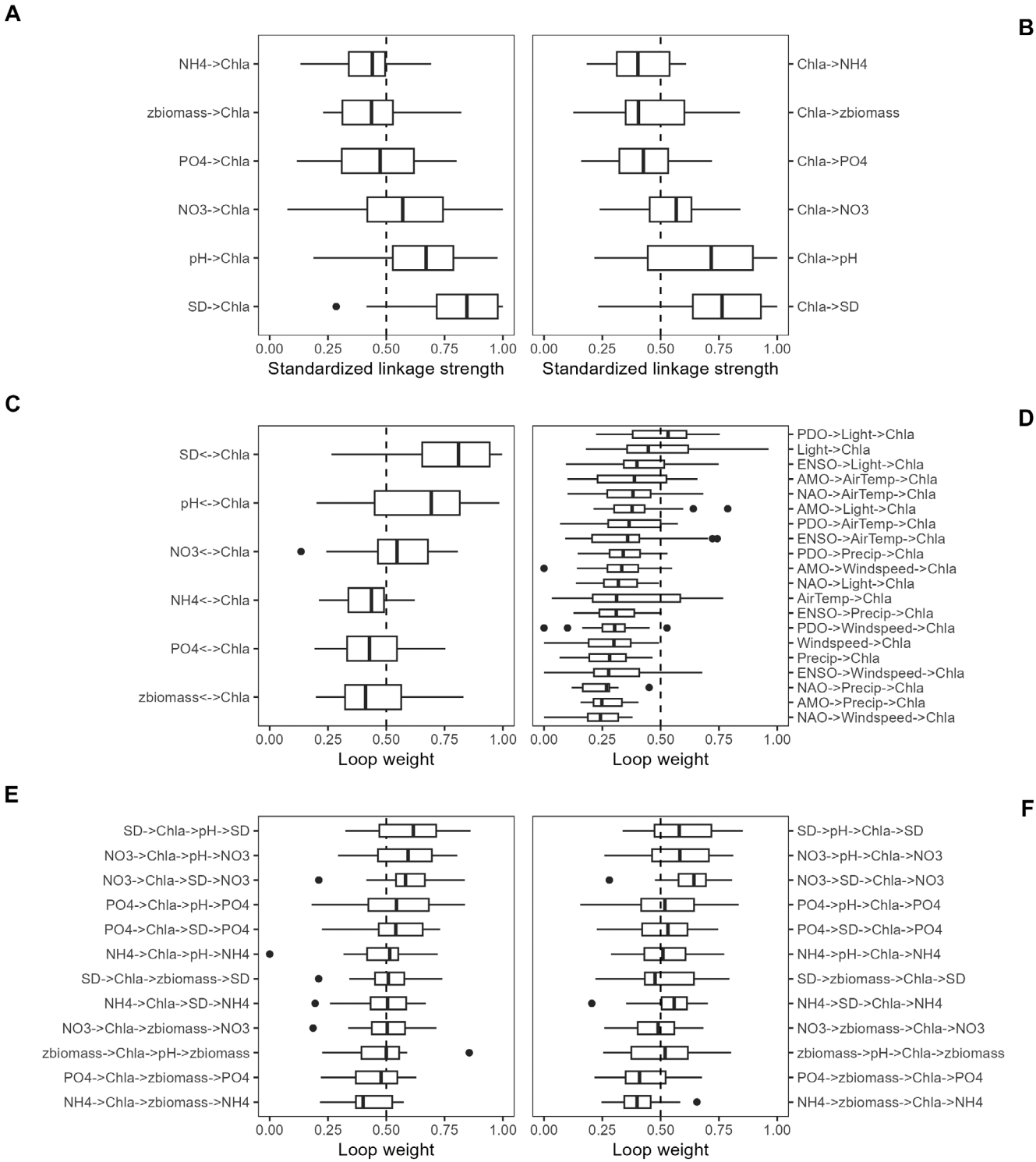

Fig. 1. Standardized linkage strength of causal linkages (**a** and **b**), loop weight of pairwise feedbacks (**c**), causal pathways (**d**), and triangle feedbacks (**e** and **f**) between the tested variables across the time series (1989–2008). Chl: chlorophyll *a*; NO_3: nitrate; NH_4: ammonium; PO_4: orthophosphate; SD: Secchi depth; zbiomass, zooplankton biomass. The loop weight ranged from 0 to 1 and the vertical line indicates a value of loop weight that is equal to 0.5.

Table 1. Spearman correlations between the strength of causal feedbacks and system properties, including mean water depth, Mann–Kendall trends in total phosphorus (TP_tau), total nitrogen (TN_tau), and air temperature (AT_tau). Italics indicates marginal relationships ($p < 0.1$). Insignificant correlation results are not shown.

	Water depth		TP_tau		TN_tau		AT_tau	
Strength of causal feedbacks	**Coefficient**	***p* Value**	**Coefficient**	***p* Value**	**Coefficient**	***p* Value**	**Coefficient**	***p* Value**
Precip → Chl *a*	−0.48	0.032						
Chl *a* → zbiomass	−0.80	0.000						
NH_4 ↔ Chl *a*	−0.71	0.001						
zbiomass ↔ Chl *a*	−0.63	0.003					*−0.39*	*0.088*
NH_4 → Chl *a* → pH → NH_4	−0.46	0.044					−0.71	0.001
NH_4 → pH → Chl *a* → NH_4	−0.53	0.018	*−0.41*	*0.077*				
NH_4 → Chl *a* → SD → NH_4	−0.43	0.060						
NO_3 → Chl *a* → zbiomass → NO_3	*−0.40*	*0.082*					−0.54	0.015
NH_4 → Chl *a* → zbiomass → NH_4	−0.85	0.000						
NH_4 → zbiomass → Chl *a* → NH_4	*−0.43*	*0.059*						
zbiomass → pH → Chl *a* → zbiomass	−0.65	0.002						
PDO → Precip → Chl *a*	−0.52	0.020						
NAO → Precip → Chl *a*	−0.58	0.009			*0.40*	*0.080*		
Chl *a* → PO_4			−0.56	0.011				
Chl *a* → pH			*−0.41*	*0.073*	*−0.39*	*0.085*	−0.47	0.036
pH → Chl *a*			−0.52	0.020	−0.47	0.039		
PO_4 ↔ Chl *a*			−0.50	0.026			*−0.41*	*0.073*
pH < –>Chl *a*			*−0.43*	*0.061*	*−0.44*	*0.056*	*−0.44*	*0.055*
PO_4 → Chl *a* → pH → PO_4			−0.57	0.010	*−0.44*	*0.055*		
NO_3 → Chl *a* → pH → NO_3			*−0.42*	*0.070*			−0.65	0.003
PO_4 → pH → Chl *a* → PO_4			−0.57	0.011	*−0.38*	*0.097*	−0.47	0.037
NO_3 → pH → Chl *a* → NO_3			*−0.44*	*0.055*	−0.45	0.047	−0.45	0.047
PO_4 → zbiomass → Chl *a* → PO_4			−0.50	0.027			−0.45	0.046
ENSO → AirTemp → Chl *a*			*−0.43*	*0.057*				
PDO → Light → Chl *a*			−0.46	0.043				
ENSO → Light → Chl *a*			−0.45	0.048				
NO_3 → Chl *a*							−0.64	0.003
zbiomass → Chl *a*							−0.53	0.019
NO_3 ↔ Chl *a*							−0.59	0.007
NO_3 → Chl *a* → SD → NO_3							−0.51	0.022
NO_3 → zbiomass → Chl *a* → NO_3							*−0.41*	*0.077*
zbiomass → Chl *a* → pH → zbiomass							*−0.41*	*0.075*
AMO → Precip → Chl *a*							*−0.44*	*0.056*

triple feedback loops (Fu et al. 2024). The relatively stronger pH- and Secchi depth-associated feedback loops indicated that phytoplankton interacts more strongly with light and pH, acting as important intermediate influential factors linking phytoplankton, nutrients, and zooplankton. This emphasizes a strong coupling effect of the physico-chemical environment, as indicated in other studies (e.g., Zhang et al. 2018; Fu et al. 2024). In addition, the high degree of positive coupling among the tested feedback loops (Supporting Information Fig. S2) demonstrated an integrative pattern as a response to a varying environment, which would leverage external environmental forces to the phytoplankton through conductive effects (through nodes and edges) between the components of the feedback loops. This feedback loop-induced leverage effect could be positive or negative—an enhanced loop promoting phytoplankton sensitive to drivers (e.g., TN, TP) or a negative regulatory loop depressing it. In our study, enhanced loops were found for the Chl *a*–TP relationships and regulatory loops for the Chl *a*–TN relationships.

Water depth was found to control the Chl *a*–TP relationship either directly or indirectly through changes in several key causal feedbacks. Deeper lakes had a lower Chl *a* per unit of TP, which is in line with previous findings (Phillips

Table 2. Chlorophyll (Chl *a*)–nutrient relationships (TP: total phosphorus, TN: total nitrogen) estimated from generalized least squared models for each lake (1989–2008).

	Chl *a*–TP					Chl *a*–TN				
Lakes	Slope	SE	*p* Value	AICc	R^2	Slope	SE	*p* Value	AICc	R^2
RAVNSO	0.08	0.13	0.502	89.98	0.36	0.1	0.22	0.629	89.1	0.36
ARRESO	0.98	0.06	<0.001	−75.89	0.66	1.45	0.11	<0.001	−0.03	0.53
FURESOEN STORESO	0.01	0.17	0.935	302.35	0.35	1.48	0.29	<0.001	276.35	0.42
OSTRUP.GUNDSOMAGLE SO	0.91	0.07	<0.001	127.58	0.62	−0.16	0.16	0.299	243.14	0.38
ENGELSHOLM SO	1.03	0.11	<0.001	174.46	0.42	−0.15	0.14	0.304	225.35	0.28
VESTERBORG SO	0.98	0.09	<0.001	123.66	0.43	−0.5	0.07	<0.001	152.72	0.35
SOGORD SO, JYLLAND	0.86	0.14	<0.001	335.74	0.39	−1.03	0.13	<0.001	302.08	0.47
NORSSO	0.55	0.10	<0.001	−103.24	0.2	0.37	0.11	0.001	−84.31	0.13
BRYRUP LANGSO	0.27	0.13	0.044	220.8	0.25	−0.81	0.14	<0.001	195.59	0.33
MAGLESO V. BRORFELDE	0.02	0.03	0.516	−79.45	0.02	0.1	0.09	0.244	−82.85	0.03
TISSO	0.26	0.09	0.006	176.74	0.17	0.06	0.12	0.573	183.66	0.15
HORNUM SO	0.93	0.12	<0.001	178.23	0.22	1.12	0.13	<0.001	170.06	0.24
SOBY SO, MIDTJYLLAND	0.69	0.11	<0.001	73.53	0.22	0.96	0.14	<0.001	74.83	0.21
ARRESKOV SO	1	0.12	<0.001	331.74	0.35	0.88	0.21	<0.001	366.99	0.24
SOHOLM SO	−0.44	0.13	0.001	151.37	0.21	−0.38	0.14	0.006	152.4	0.21
HINGE SO	1	0.14	<0.001	114.91	0.5	−0.3	0.10	0.003	147.63	0.43
KVIE SO	0.83	0.15	<0.001	235.3	0.26	1.75	0.20	<0.001	209.41	0.34
HOLM SO	0.43	0.08	<0.001	177.39	0.13	0.69	0.09	<0.001	152.62	0.21
STORE SOGORD SO	0.49	0.14	<0.001	336.26	0.23	−0.77	0.14	<0.001	317.39	0.29
UTTERSLEV MOSE	0.5	0.05	<0.001	−18.49	0.38	0.9	0.09	<0.001	−32.23	0.41

et al. 2008) and largely reflects that light limitation in deep lake weakens the response of phytoplankton to phosphorus. Notably, the causal feedback between phytoplankton and local drivers mediated the Chl *a*–TP relationship across water depth gradients, and the Chl *a*–TP slope thus increased significantly in shallow lakes. Our results demonstrated a notable self-reinforced feedback loop (e.g., $NH_4 \rightarrow$ Chl $a \rightarrow$ pH $\rightarrow NH_4$) where algae proliferation enhanced water pH and stimulated N recycling (e.g., NH_4 regenerated by waste excretions by cellular exudation, zooplankton, protists, and mineralization of organic matter by bacteria) (McCarthy et al. 2013), which was strongly coupled with the other tested feedback loops (Supporting Information Fig. S2, PO_4). Therefore, the stronger self-amplifying feedback loops in shallower lakes could be an important mechanism contributing to higher phytoplankton sensitivity to nutrients (McCarthy et al. 2013). Similar patterns were found for the causal feedbacks of phytoplankton to zooplankton, which is supported by previous findings that a TP reduction may cause a significant decline in fish biomass and thus enhanced zooplankton grazing on phytoplankton; this effect being stronger in shallow lakes (Jeppesen et al. 1997, 2005*b*). Therefore, our results suggest that prey–predator feedback may promote the phytoplankton yield per unit of TP in shallow lakes.

Long-term trends in TP indirectly had systematic effects on the Chl *a*–nutrient relationship via changes in the causal feedback. In lakes with an extensive TP reduction (TP_tau), the causal feedbacks between phytoplankton and local drivers (e.g., NH_4, pH, PO_4) tended to be stronger, strengthening the Chl *a*–TP relations and weakening the Chl *a*–TN relations. The observed self-amplifying feedback loops indicate that minor increases in loop components (e.g., Chl *a*, NH_4, pH, PO_4) would leverage phytoplankton proliferation as well as nutrient recycling (hereafter positive leverage effects) and vice versa in the case of a decrease (hereafter inverse leverage effects). In Danish lakes, previous studies have demonstrated that long-term TP reductions caused a significant decline in phytoplankton biomass (Chl *a*) and the Chl *a* : TP ratio and increases in the zooplankton : phytoplankton biomass ratio (Jeppesen et al. 2005*b*). Our findings on causal feedback may provide a mechanistic explanation of this phenomenon; that is, TP reduction triggered inverse leverage effects, which became more pronounced at increasing TP_tau, leading to a faster decrease of Chl *a* in response to TP. Also, it led to a faster decline of the Chl *a* : TP ratio (a more negative Kendall's τ), although a positive Kendall's τ of Chl *a* : TP was observed in lakes with weaker feedback loops (e.g., $NH_4 \leftrightarrow$ Chl *a*) and lower TP_tau. However, the lakes with the highest (more negative) TP_tau often had higher TP levels (indicating a negative relationship between TP_tau and mean TP values, $p < 0.001$; Supporting Information Fig. S3), which might contribute to a relatively large Chl *a*–TP slope.

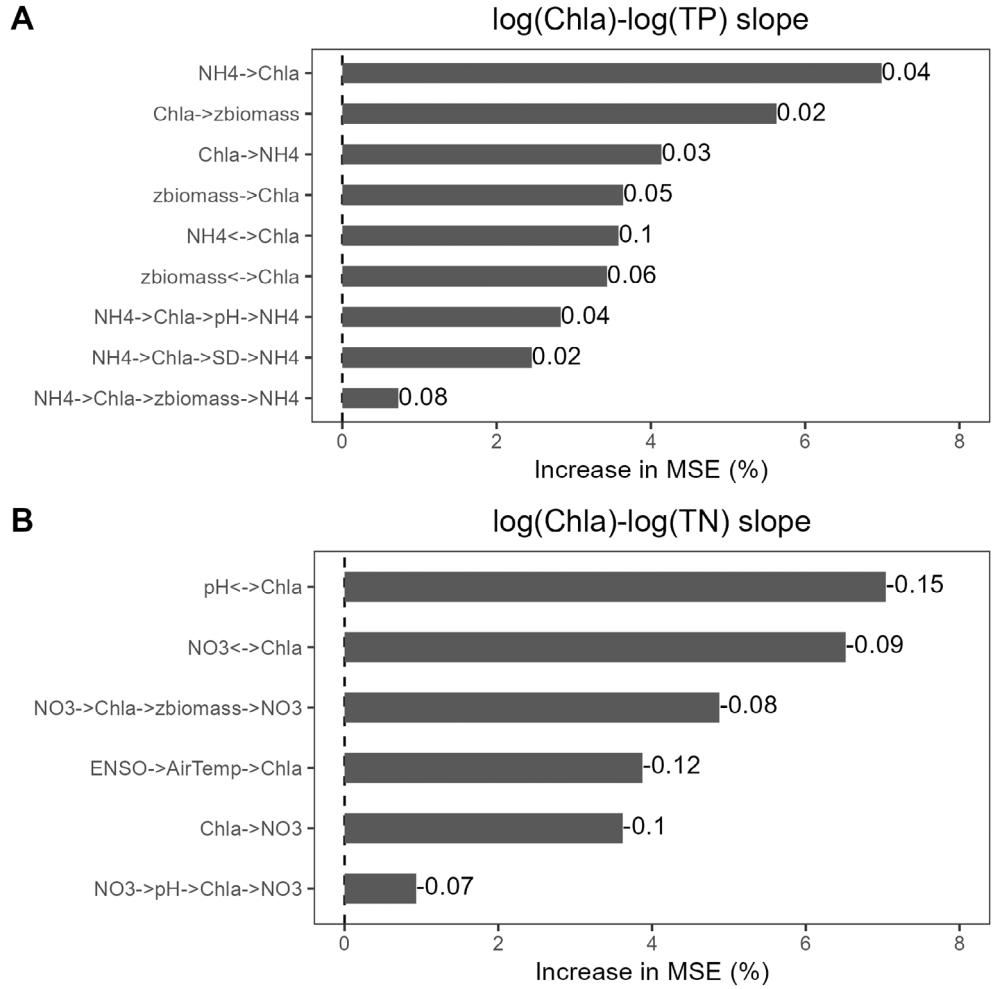

Fig. 2. Random forest regression showing mean predictor importance (percentage increase of mean square error, MSE increase) of each causal feedback in determining the log-linear relationships between phytoplankton biomass (Chl *a*) and nutrients (**a**, TP: total phosphorus; **b**, TN: total nitrogen). The numbers in the figure represent the slope for each determinant, and R^2 and *p* value for the whole model are indicated. NO_3: nitrate; NH_4: ammonium; PO_4: orthophosphate; SD: Secchi depth; zbiomass: zooplankton biomass.

In lakes with high TP_tau, in contrast, the stronger causal feedbacks of pH ↔ Chl *a* triggered by inverse leverage effects induced a shift in the Chl *a*–TN relationship from positive to negative. Previous findings have indicated a stronger response of phytoplankton to nitrogen as well as of its effect on the N recycling at high phosphorus availability (McCauley et al. 1989; Filstrup et al. 2014; Quinlan et al. 2021). This implies stronger feedback between phytoplankton and nitrogen in lakes with high TP (as well as TP_tau in Danish lakes). Although CCM cannot detect if the causal feedbacks are positive or negative (Sugihara et al. 2012), we can expect a strong negative feedback associated with nitrogen as the observed self-amplifying (positive) feedback, while phosphorus may cause accelerating P recycling as well as removal of nitrogen and thus a reduced N : P ratio (Cottingham et al. 2015). Furthermore, the more negative Chl *a*–TN slope in lakes with high TN_tau suggests that this causal feedback acts as an enhancement loop for the Chl *a*–TP relations and as a regulatory loop for the Chl *a*–TN relations, respectively.

Unlike the effects of nutrient reduction, trends toward higher warming (AT_tau) tended to weaken the causal feedback loops (e.g., $NH_4 \rightarrow$ Chl $a \rightarrow$ pH $\rightarrow NH_4$, $PO_4 \leftrightarrow$ Chl *a*, $NO_3 \leftrightarrow$ Chl *a*). Likewise, climate warming has been suggested to affect the trophic linkages between phytoplankton and zooplankton either due to mismatch in spring (Winder and Schindler 2004*b*) or to increased fish predation on zooplankton (Jeppesen et al. 2011). In addition, a warmer climate coupled with re-oligotrophication and higher water depth results in a lower hypolimnetic temperature and stronger thermal stratification (Winder and Schindler 2004*a*), which largely prevents the transport of sediment-driven nutrients between the epilimnion and the hypolimnion (Pomati et al. 2012; Flaim et al. 2016). This would slow down the nutrient

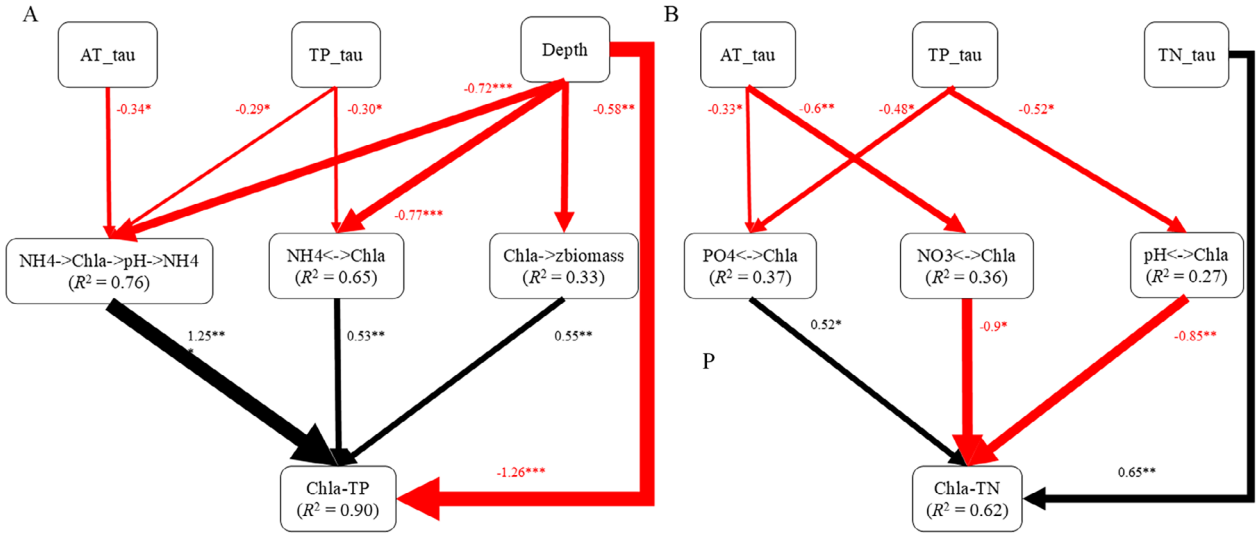

Fig. 3. Generalized multilevel path models showing the causal multivariate relationships among lake-level properties (first row), the strength of causal feedbacks (second row) and the chlorophyll *a* (Chl *a*)–TP (**a**)/TN (**b**) relationship (third row). Arrows represent the flow of causality among variables. Path coefficients (i.e., numbers associated with each arrow) are standardized partial regression coefficients. Arrow width is proportional to the standardized path coefficients. Black arrows represent positive effects and red arrows negative effects. The statistical significance for linear relationships was tested using likelihood-ratio tests. TP: total phosphorus, TN: total nitrogen, AT: air temperature, NO_3: nitrate; NH_4: ammonium; PO_4: orthophosphate; zbiomass: zooplankton biomass; *tau* indicates the coefficient of Mann–Kendall trends for TP, TN and AT across two decades (1989–2008). *$p < 0.05$; **$p < 0.01$; ***$p < 0.001$e.

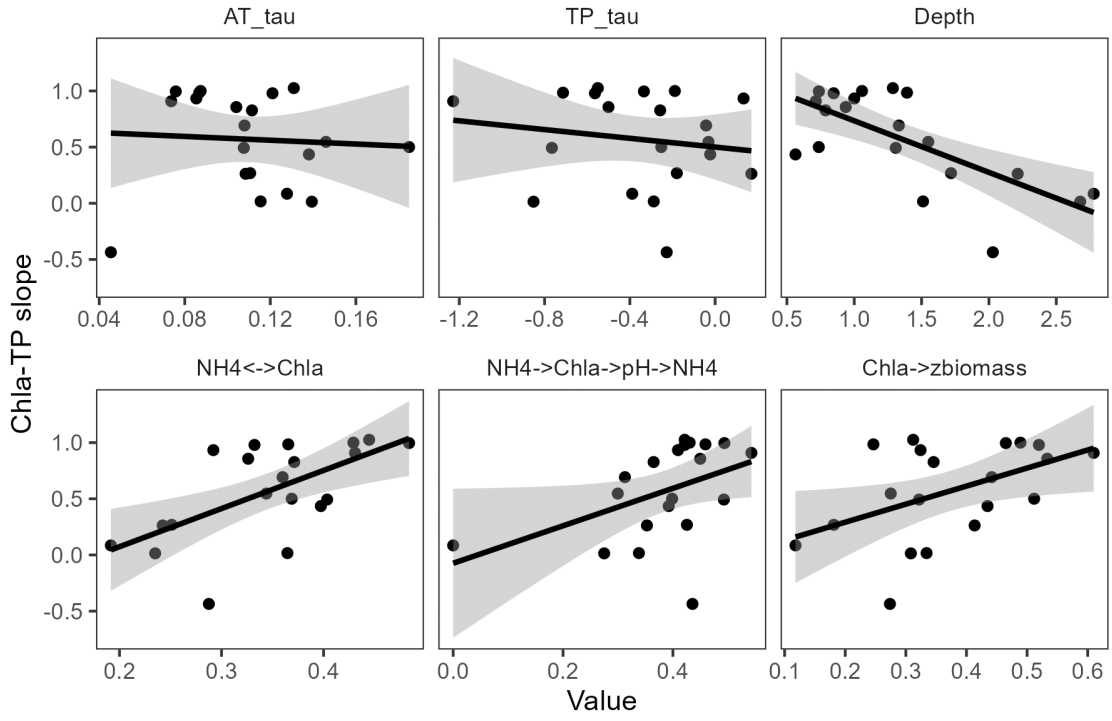

Fig. 4. Relationships between the significant drivers and the chlorophyll *a* (Chl *a*)–TP slope revealed by generalized multilevel path models. Regression lines are drawn in black. TP: total phosphorus, AT: air temperature, NH_4: ammonium; zbiomass: zooplankton biomass; *tau* indicates the coefficient of Mann–Kendall trends for TP, TN, and AT across two decades (1989–2008).

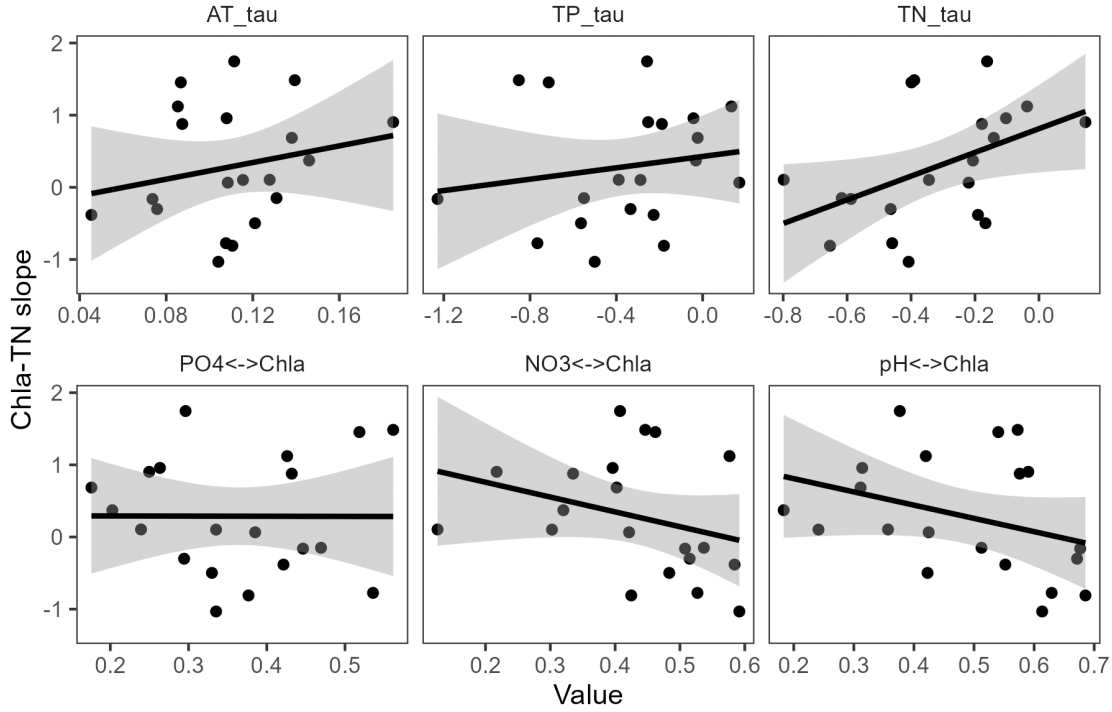

Fig. 5. Relationships between the significant drivers and chlorophyll *a* (Chl *a*)–TN slope revealed by generalized multilevel path models. Regression lines are drawn in black. TP: total phosphorus, TN: total nitrogen, AT: air temperature, NO_3: nitrate; PO_4: orthophosphate; zbiomass: zooplankton biomass; *tau* indicates the coefficient of Mann–Kendall trends for TP, TN, and AT across two decades (1989–2008).

recycling processes as well as the responses of phytoplankton to nutrients released from sediments, which ultimately dampens the enhancement loops of Chl *a*–TP relations and the regulatory loops of Chl *a*–TN relations.

Conclusion

Our results identified prevalent causal feedback loops in 20 Danish lakes, the majority of which were undergoing significant nutrient reduction and climate warming, characterized as enhancement loops for Chl *a*–TP relations and regulatory loops for Chl *a*–TN relations. The loops modified the Chl *a*–nutrient relationship in response to variations in lake system properties (e.g., depth, nutrient concentration reductions, climate warming). The enhancement feedback loops increase the extent of phytoplankton sensitivity to TP in shallow lakes with high TP reduction and a low level of warming, while the regulatory feedback loops force a shift in the Chl *a*–TN relationship from a negative slope in lakes experiencing a large nutrient reduction and a low level of warming to a positive slope in lakes with the opposite gradients. Our findings suggest a mechanistic explanation of how internal feedback loops regulate the emergent Chl *a*–nutrient relationship across a broad gradient of nutrients, warming, and lake morphology. This knowledge is useful for lake managers to advance eutrophication mitigation measures by focusing on the critical causal feedback loops as well as their components.

Data availability statement

The data that support the findings of this study are available at https://miljoedata.miljoeportal.dk (in Danish) or from the corresponding author upon a reasonable request. R code can be found on zenodo: https://zenodo.org/records/12821169.

References

Arhonditsis, G. B., M. Winder, M. T. Brett, and D. E. Schindler. 2004. Patterns and mechanisms of phytoplankton variability in Lake Washington (USA). Water Res. **38**: 4013–4027. doi:10.1016/j.watres.2004.06.030

Blenckner, T., and others. 2007. Large-scale climatic signatures in lakes across Europe: A meta-analysis. Glob. Change Biol. **13**: 1314–1326. doi:10.1111/j.1365-2486.2007.01364.x

Breiman, L. 2001. Random forests. Mach. Learn. **45**: 5–32. doi:10.1023/A:1010933404324

Cade, B. S., and B. R. Noon. 2003. A gentle introduction to quantile regression for ecologists. Front. Ecol. Environ. **1**: 412–420. doi:10.1890/1540-9295(2003)001[0412:AGITQR]2.0.CO;2

Canfield, D. E., R. W. Bachmann, M. V. Hoyer, L. S. Johansson, M. Søndergaard, and E. Jeppesen. 2019. To measure phytoplankton biovolume or chlorophyll—The aquatic conundrum with implications for the management of lakes. Lake Reserv. Manag. **35**: 181–192. doi:10.1080/10402381.2019.1607958

Carpenter, S., K. Cottingham, and D. Schindler. 1992. Biotic feedbacks in lake phosphorus cycles. Trends Ecol. Evol. **7**: 332–336. doi:10.1016/0169-5347(92)90125-U

Chang, C. W., and others. 2022. Causal networks of phytoplankton diversity and biomass are modulated by environmental context. Nat. Commun. **13**: 1140. doi:10.1038/s41467-022-28761-3

Cottingham, K. L., H. A. Ewing, M. L. Greer, C. C. Carey, and K. C. Weathers. 2015. Cyanobacteria as biological drivers of lake nitrogen and phosphorus cycling. Ecosphere **6**: 1–19. doi:10.1890/ES14-00174.1

Deng, J., H. W. Paerl, B. Qin, Y. Zhang, G. Zhu, E. Jeppesen, Y. Cai, and H. Xu. 2018. Climatically-modulated decline in wind speed may strongly affect eutrophication in shallow lakes. Sci. Total Environ. **645**: 1361–1370. doi:10.1016/j.scitotenv.2018.07.208

Filstrup, C. T., T. Wagner, P. A. Soranno, E. H. Stanley, C. A. Stow, K. E. Webster, and J. A. Downing. 2014. Regional variability among nonlinear chlorophyll—Phosphorus relationships in lakes. Limnol. Oceanogr. **59**: 1691–1703. doi:10.4319/lo.2014.59.5.1691

Flaim, G., E. Eccel, A. Zeileis, G. Toller, L. Cerasino, and U. Obertegger. 2016. Effects of re-oligotrophication and climate change on lake thermal structure. Freshw. Biol. **61**: 1802–1814. doi:10.1111/fwb.12819

Fu, H., G. Yuan, K. Özkan, L. S. Johansson, M. Søndergaard, T. L. Lauridsen, and E. Jeppesen. 2020. Seasonal and long-term trends in the spatial heterogeneity of lake phytoplankton communities over two decades of restoration and climate change. Sci. Total Environ. **748**: 141106. doi:10.1016/j.scitotenv.2020.141106

Fu, H., L. Chen, Y. Ge, A. Wu, H. Liu, W. Li, G. Yuan, and E. Jeppesen. 2022. Linking human activities and global climatic oscillation to phytoplankton dynamics in a subtrophic lake. Water Res. **208**: 117866. doi:10.1016/j.watres.2021.117866

Fu, H., and others. 2024. Weakened casualcausal feedback loops following intensive restoration efforts and climate changes in a large shallow freshwater lake. Sci. Total Environ. **913**: 169601. doi:10.1016/j.scitotenv.2023.169601

Gao, Y., J. C. Cornwell, D. K. Stoecker, and M. S. Owensp. 2014. Influence of cyanobacteria blooms on sediment biogeochemistry and nutrient fluxes. Limnol. Oceanogr. **59**: 959–971. doi:10.4319/lo.2014.59.3.0959

Grace, J. B., and K. A. Bollen. 2005. Interpreting the results from multiple regression and structural equation models. Bull. Ecol. Soc. Am. **86**: 283–295. doi:10.1890/0012-9623(2005)86[283:ITRFMR]2.0.CO;2

Huisman, J., G. A. Codd, H. W. Paerl, B. W. Ibelings, J. M. H. Verspagen, and P. M. Visser. 2018. Cyanobacterial blooms. Nat. Rev. Microbiol. **16**: 471–483. doi:10.1038/s41579-018-0040-1

Jeppesen, E., J. P. Jensen, M. Søndergaard, T. Lauridsen, L. J. Pedersen, and L. Jensen. 1997. Top-down control in freshwater lakes: The role of nutrient state, submerged macrophytes and water depth. Hydrobiologia **342**: 151–164. doi:10.1023/a:1017046130329

Jeppesen, E., J. P. Jensen, M. Søndergaard, and T. L. Lauridsen. 2005*a*. Response of fish and plankton to nutrient loading reduction in eight shallow Danish lakes with special emphasis on seasonal dynamics. Freshw. Biol. **50**: 1616–1627. doi:10.1111/j.1365-2427.2005.01413.x

Jeppesen, E., and others. 2005*b*. Lake responses to reduced nutrient loading—an analysis of contemporary long-term data from 35 case studies. Freshw. Biol. **50**: 1747–1771. doi:10.1111/j.1365-2427.2005.01415.x

Jeppesen, E., and others. 2011. Zooplankton as indicators in lakes: A scientific-based plea for including zooplankton in the ecological quality assessment of lakes according to the European Water Framework Directive (WFD). Hydrobiologia **676**: 279–297. doi:10.1007/s10750-011-0831-0

Lefcheck, J. S. 2016. piecewiseSEM: Piecewise structural equation modelling in r for ecology, evolution, and systematics. Methods Ecol. Evol. **7**: 573–579. doi:10.1111/2041-210X.12512

Lu, B., and J. Hardin. 2021. A unified framework for random forest prediction error estimation. J. Mach. Learn. Res. **22**: 1–41. doi:10.5555/3546258.3546266

McCarthy, M. J., W. S. Gardner, M. F. Lehmann, and D. F. Bird. 2013. Implications of water column ammonium uptake and regeneration for the nitrogen budget in temperate, eutrophic Missisquoi Bay, Lake Champlain (Canada/USA). Hydrobiologia **718**: 173–188. doi:10.1007/s10750-013-1614-6

McCauley, E., J. A. Downing, and S. Watson. 1989. Sigmoid relationships between nutrients and chlorophyll among lakes. Can. J. Fish. Aquat. Sci. **46**: 1171–1175. doi:10.1139/f89-152

Meerhoff, M., and others. 2022. Feedback between climate change and eutrophication: Revisiting the allied attack concept and how to strike back. Inland Waters **12**: 187–204. doi:10.1080/20442041.2022.2029317

O'brien, R. M. 2007. A caution regarding rules of thumb for variance inflation factors. Qual. Quant. **41**: 673–690. doi:10.1007/s11135-006-9018-6

Olson, C. R., and S. E. Jones. 2022. Chlorophyll–total phosphorus relationships emerge from multiscale interactions from algae to catchments. Limnol. Oceanogr.: Lett. **7**: 483–491. doi:10.1002/lol2.10281

Özkan, K., E. Jeppesen, T. A. Davidson, M. Søndergaard, T. L. Lauridsen, R. Bjerring, L. S. Johansson, and J.-C. Svenning. 2014. Cross-taxon congruence in lake plankton largely independent of environmental gradients. Ecology **95**: 2778–2788. doi:10.1890/13-2141.1

Paerl, H. W., and T. G. Otten. 2013*a*. Blooms bite the hand that feeds them. Science **342**: 433–434. doi:10.1126/science.1245276

Paerl, H. W., and T. G. Otten. 2013*b*. Harmful cyanobacterial blooms: Causes, consequences, and controls. Microb. Ecol. **65**: 995–1010. doi:10.1007/s00248-012-0159-y

Paerl, H. W., and others. 2016. It takes two to tango: When and where dual nutrient (N & P) reductions are needed to

protect lakes and downstream ecosystems. Environ. Sci. Technol. **50**: 10805–10813. doi:10.1021/acs.est.6b02575

Phillips, G., O.-P. Pietiläinen, L. Carvalho, A. Solimini, A. Lyche Solheim, and A. C. Cardoso. 2008. Chlorophyll–nutrient relationships of different lake types using a large European dataset. Aquat. Ecol. **42**: 213–226. doi:10.1007/s10452-008-9180-0

Pomati, F., B. Matthews, J. Jokela, A. Schildknecht, and B. W. Ibelings. 2012. Effects of re-oligotrophication and climate warming on plankton richness and community stability in a deep mesotrophic lake. Oikos **121**: 1317–1327. doi:10.1111/j.1600-0706.2011.20055.x

Prairie, Y. T., C. M. Duarte, and J. Kalff. 1989. Unifying nutrient–chlorophyll relationships in lakes. Can. J. Fish. Aquat. Sci. **46**: 1176–1182. doi:10.1139/f89-153

Prepas, E. E., and D. O. Trew. 1983. Evaluation of the phosphorus–chlorophyll relationship for lakes off the Precambrian Shield in western Canada. Can. J. Fish. Aquat. Sci. **40**: 27–35. doi:10.1139/f83-005

Qin, B., and others. 2019. Why Lake Taihu continues to be plagued with cyanobacterial blooms through 10 years (2007–2017) efforts. Sci. Bull. **64**: 354–356. doi:10.1016/j.scib.2019.02.008

Quinlan, R., and others. 2021. Relationships of total phosphorus and chlorophyll in lakes worldwide. Limnol. Oceanogr. **66**: 392–404. doi:10.1002/lno.11611

R Core Team. 2013. R: A language and environment for statistical computing. https://www.r-project.org/

Scheffer, M., S. H. Hosper, M. L. Meijer, B. Moss, and E. Jeppesen. 1993. Alternative equilibria in shallow lakes. Trends Ecol. Evol. **8**: 275–279. doi:10.1016/0169-5347(93)90254-M

Schindler, D. W., S. R. Carpenter, S. C. Chapra, R. E. Hecky, and D. M. Orihel. 2016. Reducing phosphorus to curb lake eutrophication is a success. Environ. Sci. Technol. **50**: 8923–8929. doi:10.1021/acs.est.6b02204

Shipley, B. 2009. Confirmatory path analysis in a generalized multilevel context. Ecology **90**: 363–368. doi:10.1890/08-1034.1

Shipley, B. 2013. The AIC model selection method applied to path analytic models compared using ad-separation test. Ecology **94**: 560–564. doi:10.1890/12-0976.1

Smith, V. H., and D. W. Schindler. 2009. Eutrophication science: Where do we go from here? Trends Ecol. Evol. **24**: 201–207. doi:10.1016/j.tree.2008.11.009

Sugihara, G., R. May, H. Ye, C.-H. Hsieh, E. Deyle, M. Fogarty, and S. Munch. 2012. Detecting causality in complex ecosystems. Science **338**: 496–500. doi:10.1126/science.1227079

Takens, F. 1981. Detecting strange attractors in turbulence, p. 366–381. *In* D. Rand and L. S. Young [eds.], Dynamical systems and turbulence, Warwick 1980, v. **898**. Springer. doi:10.1007/BFb0091924

Winder, M., and D. E. Schindler. 2004*a*. Climatic effects on the phenology of lake processes. Glob. Change Biol. **10**: 1844–1856. doi:10.1111/j.1365-2486.2004.00849.x

Winder, M., and D. E. Schindler. 2004*b*. Climate change uncouples trophic interactions in an aquatic ecosystem. Ecology **85**: 2100–2106. doi:10.1890/04-0151

Wu, B., and others. 2022. Chlorophyll-nutrient relationship changes with lake type, season and small-bodied zooplankton in a set of subtropical shallow lakes. Ecol. Indic. **135**: 108571. doi:10.1016/j.ecolind.2022.108571

Xiao, X., J. He, Y. Yu, B. Cazelles, M. Li, Q. Jiang, and C. Xu. 2019. Teleconnection between phytoplankton dynamics in north temperate lakes and global climatic oscillation by time-frequency analysis. Water Res. **154**: 267–276. doi:10.1016/j.watres.2019.01.056

Yan, X., and others. 2017. Climate warming and cyanobacteria blooms: Looks at their relationships from a new perspective. Water Res. **125**: 449–457. doi:10.1016/j.watres.2017.09.008

Ye, H., A. Clark, E. Deyle, and G. Sugihara. 2016. rEDM: An R package for empirical dynamic modeling and convergent cross-mapping. cran.r-project.org. https://CRAN.R-project.org/package=rEDM

Yuan, L. L., and J. R. Jones. 2020. Rethinking phosphorus–chlorophyll relationships in lakes. Limnol. Oceanogr. **65**: 1847–1857. doi:10.1002/lno.11422

Zhang, Y., B. Qin, G. Zhu, K. Shi, and Y. Zhou. 2018. Profound changes in the physical environment of Lake Taihu from 25 years of long-term observations: Implications for algal bloom outbreaks and aquatic macrophyte loss. Water Resour. Res. **54**: 4319–4331. doi:10.1029/2017WR022401

Zhao, L., R. Zhu, Q. Zhou, E. Jeppesen, and K. Yang. 2023. Trophic status and lake depth play important roles in determining the nutrient-chlorophyll *a* relationship: Evidence from thousands of lakes globally. Water Res. **242**: 120182. doi:10.1016/j.watres.2023.120182

Zou, W., G. Zhu, H. Xu, M. Zhu, Y. Zhang, and B. Qin. 2022. Temporal dependence of chlorophyll *a*–nutrient relationships in Lake Taihu: Drivers and management implications. J. Environ. Manag. **306**: 114476. doi:10.1016/j.jenvman.2022.114476

Acknowledgments

This study was supported by the National Natural Science Foundation of China (Grant No. 32371642) and the Natural Science Foundation of Hunan Province of China (Grant No. 2021JJ20031). EJ and KÖ were supported by the TÜBITAK BIDEB2232 program (project 118C250). MS was supported by the Poul Due Jensen Foundation. We thank Anne Mette Poulsen for the English revision.

Conflict of Interest

None declared.

Submitted 06 February 2024
Revised 30 May 2024
Accepted 06 August 2024

Associate editor: Grace M. Wilkinson